



# Water Use of Hybrid Poplar (*Populus deltoides* Bart. ex Marsh × *P. nigra* L. “AF2”) Growing Across Contrasting Site and Groundwater Conditions in Western Slovakia

Gabriela Fontenla-Razzetto<sup>1</sup> · Filipa Tavares Wahren<sup>1</sup> · Dávid Heilig<sup>2</sup> · Bálint Heil<sup>2</sup> · Gábor Kovacs<sup>2</sup> · Karl-Heinz Feger<sup>1</sup> · Stefan Julich<sup>1</sup>

Received: 22 December 2021 / Accepted: 28 March 2022  
© The Author(s) 2022

## Abstract

The water use by short rotation coppices (SRC) has been a focus of ongoing research in the last decades. Nevertheless, investigations that consider site factors and present long-term monitoring of the components of the water balance are rare. This research quantified the tree-based transpiration in the 4th growing season of uncoppiced 1st rotational hybrid poplar stands (*Populus deltoides* Bart. ex Marsh × *P. nigra* L. “AF2”) in western Slovakia. The aim of the study was to determine the influence of meteorological and soil-related site conditions on transpiration rates. Three experimental plots were located in the Morava River floodplains, on loamy sand-textured soils with different groundwater accessibilities: higher, low, and fluctuating groundwater level. We measured sap flow (Heat Ratio Method), volumetric water content, matric potential, groundwater level, and meteorological variables throughout the growing season in 2019. The results indicated that transpiration in the three sites was almost constant during that period, which was characterized by distinct conditions. The average cumulative transpiration at the site with a higher groundwater level (1105 mm) was larger than at the site with a lower groundwater level (632 mm) and the site with fluctuating groundwater (863 mm). A principal component analysis (PCA) and correlation analysis identified that the contribution of meteorological and soil-related site variables to transpiration differed among the sites. Soil water availability and groundwater accessibility are critical variables for the water use of poplar SRC. We concluded that the combination of site conditions needs to be reconsidered for the expansion of sustainable short rotation plantations in Europe.

**Keywords** Short rotation coppices (SRC) · Poplar · Sap flow · Transpiration · Site conditions

## Introduction

In the context of the European Green Deal, the European Union has raised its ambition to reduce greenhouse gas (GHG) emissions by at least 55% in comparison to the levels of 1990 [1]. The use of bioenergy, including woody biomass sources, is a key component for achieving these EU targets [2]. Short rotation coppices (SRC), in particular,

can efficiently contribute to the reduction of GHG emissions and can simultaneously provide significant co-benefits like habitats for flora and fauna and erosion control [3]. Short rotation coppices grow under intensive silvicultural management, and they include fast-growing tree species such as poplars (*Populus* spp.) and willows (*Salix* spp.). As of 2017, approximately 50,000 hectares of SRC have been established in Europe [4, 5]. One advantage of SRC is their cultivation on marginal or abandoned lands; it can extend over areas which are not in use for food production [6]. Regardless of the positive impacts of SRC, there are still concerns associated with their potential high water consumption [7, 8] and the possible related decline in groundwater levels [9].

The water use of SRC, specifically that of poplars, has been the focus of research in Europe, China, the USA, and Canada in the last 25 years (e.g., [10, 11]). Studies often refer to high-density, multi-stemmed coppiced SRC

✉ Gabriela Fontenla-Razzetto  
gabriela.fontenla\_razzetto2@tu-dresden.de

<sup>1</sup> Institute of Soil Science and Site Ecology, Faculty of Environmental Sciences, Technische Universität Dresden, Tharandt, Germany

<sup>2</sup> Institute of Environmental and Earth Sciences, Faculty of Forestry, University of Sopron, Ökoforestino Kft., Ibolya út 1 1. V/21, Sopron, Hungary

plantations, whereas young, uncoppiced, single-stem poplars on low-density plantations are understudied (cf [12]). Most studies were conducted during short time periods that did not cover the full growing season [13–16] with a few exceptions [8, 17]. Furthermore, for adequate quantification of SRC poplar transpiration, careful consideration of local site conditions and the planted hybrid is necessary [18, 19]. The transferability of results from one area to another is not a straightforward process [20]. Hence, the consideration of site-specific factors in the study of water use of SRC plantations in marginal land in Europe has become increasingly relevant.

Our research aimed to determine (tree-based) transpiration of the hybrid poplar “AF2” (*Populus deltoides* Bart. ex Marsh  $\times$  *P. nigra* L.) at selected sites in western Slovakia. The experimental plots had comparable soil texture and only differed in their groundwater accessibility. At the time of the study, all stands were in their 4th growing season. To our knowledge, water-related research on clone “AF2” including long-term monitoring is inexistent for these site characteristics. Such studies are needed to quantify the potential impacts of different hybrid poplars on water balance and could contribute useful information

for plantation managers with focus on bioenergy and other ecosystem services.

The objectives of the research were (1) to quantify the water use of clone “AF2” in a young, low-density, uncoppiced plantation on sites with contrasting groundwater conditions and (2) to determine the influence of meteorological (vapor pressure deficit, photosynthetic active radiation) and soil-related site conditions (groundwater, soil moisture, and matric potential) on transpiration. We hypothesized that there were differences in transpiration rates among the stands based on soil water conditions and accessibility to groundwater. Furthermore, we expected the influence of the meteorological conditions in transpiration to be limited by the different soil-related site conditions.

## Materials and Methods

### Study Area

The study area is located near the village of Kopčany, Skalica region, western Slovakia (Fig. 1). The elevation is about 170 m.a.s.l. and has a predominantly plane topography.

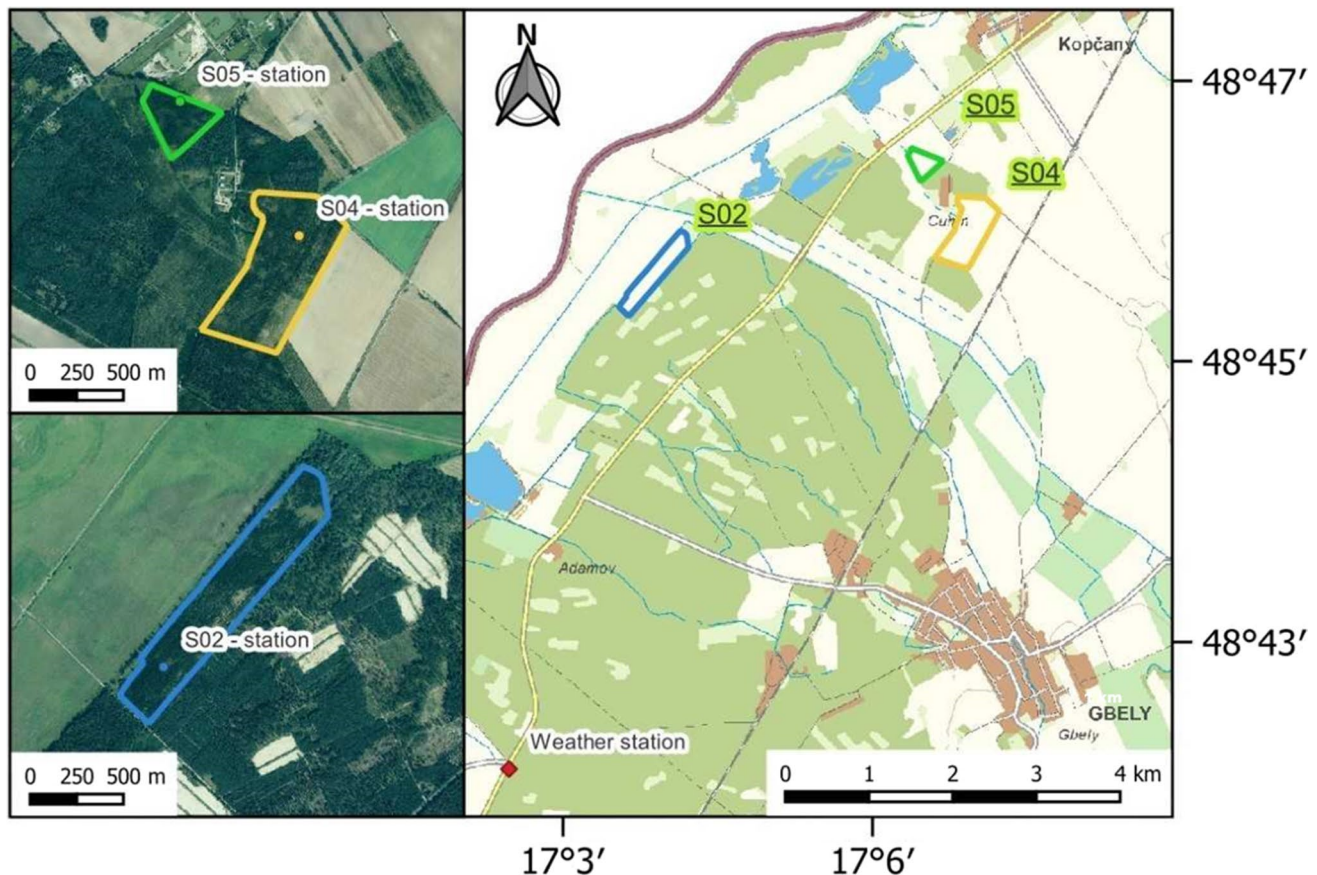


**Fig. 1** Location of study area and experimental plots near the village of Kopčany, Skalica region, western Slovakia

The climate is classified as continental climate with warm summers. Weather records from the period 1982–2012 [21] (Table 1) indicate a mean annual air temperature of 10.4 °C, with an average of 17 °C in the growing season. Mean annual precipitation is 518 mm with minimum and

maximum precipitation occurring in February and June, respectively.

The three selected hybrid poplar stands are located in the floodplains of the Morava River (Fig. 1). The plot selection followed a gradient of groundwater accessibility based on mean annual depths of the water table below the surface: (1) site S5-N, with higher groundwater level located at  $1.93 \pm 0.16$  m; (2) site S4-D, with low groundwater level located at  $3.29 \pm 0.22$  m; and (3) site S2-F, with fluctuating groundwater that ranged from 1.18 to 1.77 m and had a mean of  $1.55 \pm 0.13$  m (Table 2). For the determination of soil texture, we collected composite soil samples at 30-, 60-, and 90-cm soil depth in a representative location at each plot. The soil analyses were performed at the Institute of Soil Science and Site Ecology, TU Dresden (TUD-ISSE). Samples were air-dried at room temperature and passed through a 2-mm sieve. Air-dried disturbed samples were used to determine soil texture as well as carbon (C) and nitrogen (N) contents. Soil texture of the fraction < 2 mm was determined

**Table 1** Meteorological conditions during study period in 2019 (DOY 115–273) as compared to long-term averages (periods 1982–2012) [21]

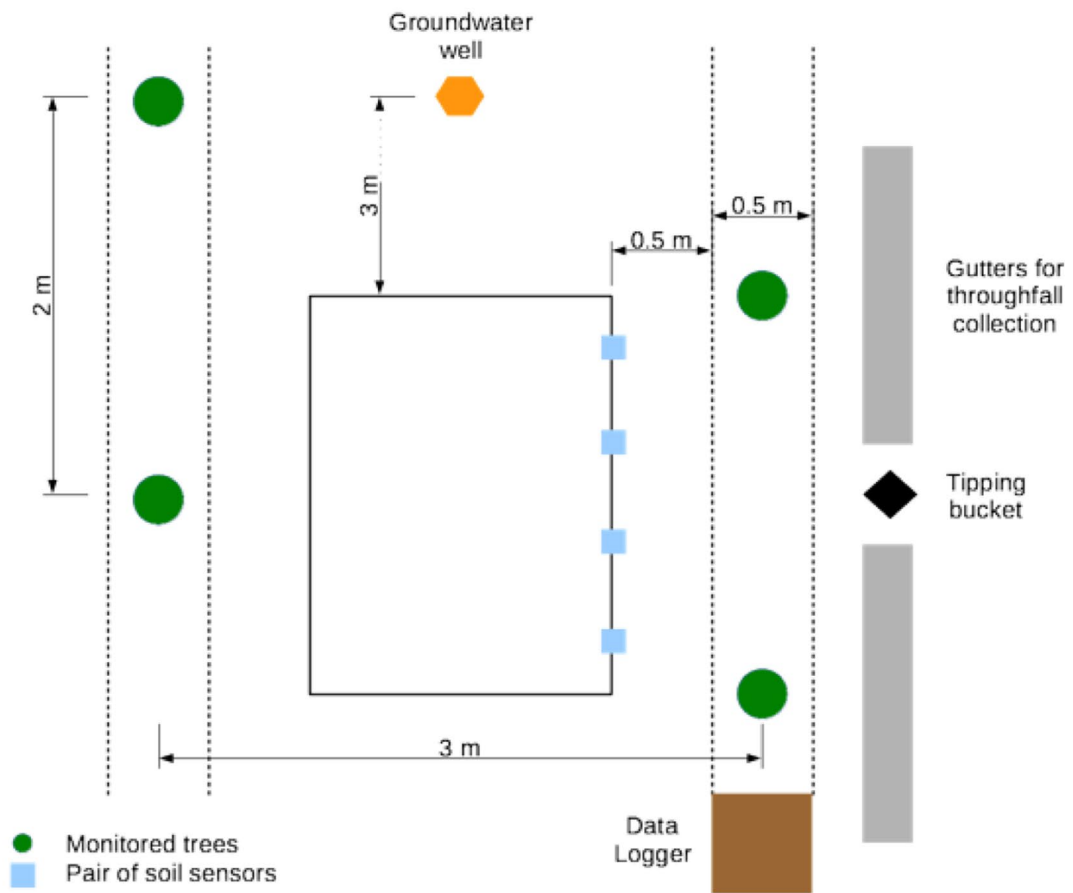
	Precipitation [mm]		Temperature [°C]	
	1982–2012	2019	1982–2012	2019
May	67	129	14.3	12.2
Jun	86	32	17.7	22.0
Jul	83	35	19.1	20.4
Aug	77	53	18.8	21.2
Sep	49	52	15.1	15.0

**Table 2** Site location and characteristics of the three experimental plots within study area (GW groundwater level measured during the growing season 2019)

Site	Location	Site parameters	Sand (mass-%)	Silt (mass-%)	Clay (mass-%)	Gravel (vol-%)	Total C (%)	Total N (%)
Site S5-N (higher groundwater level)	48.46908°N, 17.54941°E							
Mean GW level (m below surface)		$1.9 \pm 0.16$						
Plantation area (ha) (*)		8.09						
Tree mean DBH (cm) (*)		$9.5 (\pm 2.6)$						
Tree mean height (m) (*)		$6.8 (\pm 1.0)$						
Soil at 30 cm			71.7	17.6	10.7	3.6	1.20	0.10
Soil at 60 cm			71.1	17.6	11.4	16.0	0.94	0.07
Soil at 90 cm			78.0	13.9	8.1	52.0	0.31	0.02
Site S4-D (low groundwater level)	48.455190°N, 17.62880°E							
Mean GW level (m below surface)		$3.3 \pm 0.22$						
Plantation area (ha) (*)		34.32						
Tree mean DBH (cm) (*)		$5.5 (\pm 1.9)$						
Tree mean height (m) (*)		$3.3 (\pm 0.1)$						
Soil at 30 cm			90.7	5.1	4.2	1.9	0.43	0.04
Soil at 60 cm			87.3	4.9	8.2	0.4	0.10	0.02
Soil at 90 cm			88.7	6.0	5.3	1.2	0.04	0.01
Site S2-F (fluctuating groundwater level)	48.45260°N, 17.3690°E							
Mean GW level (m below surface)		1.18–1.77						
Plantation area (ha) (*)		22.74						
Tree mean DBH (cm) (*)		$8.2 (\pm 2.1)$						
Tree mean height (m) (*)		$4.5 (\pm 1.5)$						
Soil at 30 cm			83.7	12.6	3.8	5.3	0.73	0.07
Soil at 60 cm			87.6	10.4	2.6	14.0	0.12	0.01
Soil at 90 cm			94.7	3.7	1.9	3.9	0.10	0.01

(\*) Forest inventory 2017–2018 [22]

**a** TOP VIEW



**b**

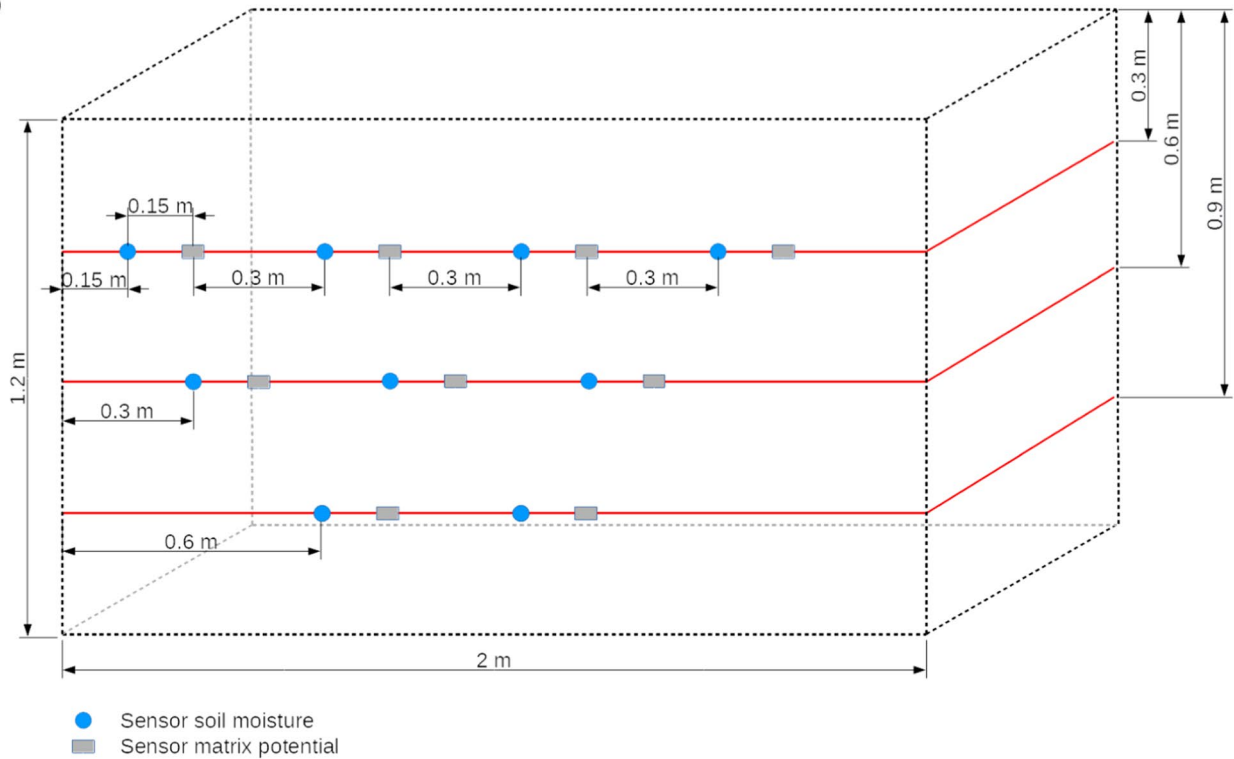


**Fig. 2 a** Schematic top view of the experimental plot, including monitored trees and groundwater well. **b** Distribution of sensors of soil moisture and matric potential in the soil profile pit at each site. At the site with low groundwater table (S4-D), the first sensor row was installed at 25-cm soil depth to avoid the limit with the next horizon. At the site with fluctuating groundwater level (S2-F), at 90-cm soil depth, high gravel content prevented the installation of matric potential sensors

by combined sieving and sedimentation analysis. Prior to the analysis, organic matter was removed by adding hydrogen peroxide, and particles were dispersed by adding sodium diphosphate. C and N concentrations in the air-dried soil material were measured with the Vario TOC™ cube (Elementar, Hanau, Germany). Soils were categorized as loamy sands, with more than 70% sand, low water-holding capacities, and poor structure (Table 2). The proportion of silt and clay at the site with higher groundwater level (S5-N) was larger than at the other two sites.

Prior to the establishment of the SRC plantations, the areas were categorized as marginal lands. The SRC plantations were established in 2016 with the hybrid “AF2” (*Populus deltoides* Bart. ex Marsh × *P. nigra* L.) in a planting grid of 3 m × 2 m (1667 trees ha<sup>-1</sup>). At the time of the study, the stands were in their fourth growing year, and the tree individuals were not coppiced. Mechanical weed control (i.e., disking) is the only management intervention at all sites, and fertilization is not applied. According to a forest inventory done in 2017–2018 based on the principles of Hartmann [22], mean tree height was 3.3 m ± 1.0 m at the site S4-D (low groundwater level), whereas at the site S5-N (higher groundwater level), this value was 6.8 ± 1.0 m. At the site S2-F (fluctuating groundwater level), mean tree height was 4.5 ± 1.5 m (Table 2).

## Instrumentation and Continuous Field Measurements

### Meteorological Station

A meteorological station was installed in June 2018 southwest of the experimental plots (48.415725°N, 17.22581°E) (Fig. 1). It included a pyranometer sensor (SP-110 Apogee) for the measurement of global radiation. Air temperature, relative humidity, air pressure, wind direction, and velocity were monitored with a Luft Sensor WS500-UMB. Rainfall was recorded using a Kalyx-Rainfall Sensor (EML Ltd.) with a receiver tank with an area of 127 cm<sup>2</sup> and a resolution of 0.2 mm per tip. Weather variables were recorded at a 30-min resolution. The distance from the meteorological station to the experimental plots was 6.57 km to site S2-F (fluctuating groundwater table), 9.56 km to site S5-N (higher groundwater table), and 9.82 km to site S4-D (low

groundwater table). The weather conditions during the growing season 2019 are summarized in Table 1.

### Soil Monitoring

A soil profile pit (1.5 m width × 2 m length × 1.5 m depth) was excavated on a representative plot at each site. Prior to the excavation of the pits, soil homogeneity for each pit was evaluated via four Pürckhauer augering profiles at 15 m distance to the pit in the four cardinal directions. The soil pits were situated between two tree rows, with an approximate distance of 0.5 m from the furrow (Fig. 2a). After excavation, the profile side of each soil pit was prepared for the installation of FDR soil moisture sensors (SM150T, Delta-T Devices) and matric potential sensors (TensioMARK, ecoTech®). Prior to the insertion of the matric potential sensors, holes were filled with a slurring suspension to allow an optimal connection between the sensor head and the soil matrix. At 30-, 60-, and 90-cm soil depths, sensors were installed in pairs (Fig. 2b). Each pair comprised a sensor for soil matric potential and a sensor for volumetric soil moisture. The distance between these two sensors was 15 cm and 30 cm between pairs. The fluctuations of the groundwater table were measured on all three sites. For that, one groundwater well per site was drilled at a 3-m distance from the soil pits. The wells had a depth of 7 m and were equipped with KELLER pressure sensors type PR-46X. Soil and groundwater data were recorded in 15-min increments. All data were stored in GP2-Delta Link dataloggers.

### Sap Flow Measurements with the Heat Ratio Method (HRM)

**Field Installation** The information of a forest inventory carried out in 2017–2018 allowed the grouping of the trees in each site into classes of diameter at breast height (DBH) (see Supporting Information Table S1 and Figure S2, Figure S3). This served as basis for the selection of the trees for the installation of the sap flow measurement devices. DBH was normally distributed at all three sites. The site with higher groundwater level (S5-N) presented larger DBH values and the site with low groundwater level (S4-D) smaller DBH. Subsequently, four trees per site were selected for the installation of the sap flow devices based on the following criteria: (1) two devices were installed within the most common DBH class at each site, (2) one device was installed in the immediately smaller DBH class, and (3) one device was installed in the immediately larger DBH class. By doing so, we aimed at capturing the diameter variability of the full stands. Additional criteria were (1) location of the trees near the soil monitoring pit and (2) enough distance to the plantation fence to reduce edge effects. The criteria were met fully at the site with higher groundwater level (S5-N). At the site with low groundwater level (S4-D), two devices had to

be installed in trees with diameters belonging to the larger DBH class, whereas at the site with fluctuating groundwater level (S2-F), it was not possible to find a second tree with a diameter within the most frequent DBH class and in the vicinity of the soil pit. Therefore, two trees were selected within the DBH class with larger diameters (Table 3).

**Heat Ratio Method (HRM)** Sap flow measurements were conducted using the heat ratio method (HRM) [23]. The HRM is a heat pulse method that measures the ratio of the increase in temperature at points equidistant downstream and upstream from a line heater. One sap flow device (ICT International, Australia) was installed per tree. Each device consisted of a set of two measuring needles and one line heater covering a xylem depth of 35 mm. Each metal needle measured at two different points, which allowed the detection of radial gradients and more precise measurements. The devices were installed after careful removal of the bark, following the manufacturer's specifications [24]. The vertical distance between needles was 1.5 cm, and they were oriented to the north. The needles were inserted radially at 1.30 m tree height on each tree. By doing so, we aimed at keeping consistency with the biometric measurements recorded in the field. Other studies installed sap flow devices at breast height or similar heights [12, 17, 25], which makes our research comparable. The sap flow measurements were conducted throughout the growing season in 2019 from bud burst (DOY 115) until end of the growing season (DOY 273), for a total of 159 days. Sap flow data were recorded at 20-min resolution in the needle temperature mode. The data were downloaded manually during periodic field visits throughout the growing season. Each visit included the measurement of the circumference at breast height at 1.30 m (CBH) at each monitored tree. For that, a forestry circumference tape

measure (1 mm accuracy) was used. Tree diameter at breast height was derived from the measured CBH and used for further data analysis. Due to technical disturbances, data gaps occurred in some of the monitored trees. Hence, monitored trees with a data gap larger than 30% of the length of the growing season were not considered for further statistical analysis. Three trees at the site with higher groundwater level (S5-N), four trees at the site with low groundwater level (S4-D), and three trees at the site with fluctuating groundwater level (S2-F) were selected for the statistical analysis and are discussed in the “Results” and “Discussion” sections.

### Estimation of the Leaf Area Index from Sentinel images

The European Space Agency Sentinel-2A Imagery Level-1C Product (cf. [26]) was used to obtain an estimation of the Leaf Area Index (LAI) at all sites. These images were atmospherically corrected by using the procedure available in the Sentinel-2 SNAP toolbox [27]. During the growing season of 2019, five Sentinel-2 overflights over the monitoring sites could be used in the assessment, and during the growing season of 2020, six overflights, having a minimum of 5% cloud coverage, were obtained. Overall, we believe the LAI product has given an underestimation of the actual tree LAI. This is reasonable, since remote sensing observations are strongly scale-dependent, complicating direct access to LAI due to the possible heterogeneity in leaf distribution within the canopy volume. Still, the obtained imagery results depict the LAI dynamics during the growing season. The minimum LAI ( $0.5 \text{ m}^2 \text{ m}^{-2}$ ) occurred at the beginning of the growing season, and maximum LAI values [ $6.4 \text{ m}^2 \text{ m}^{-2}$  for both sites S5-N (high groundwater level) and S2-F (fluctuating groundwater level);  $4.8 \text{ m}^2 \text{ m}^{-2}$  for site S4-D (low groundwater level)] occurred at the peak of the growing season.

**Table 3** Diameter at breast height (DBH, in cm) of monitored trees at time of installation and removal of sap flow meters. DBH classes (in 1 cm distribution) for monitored trees within the site with higher groundwater level (S5-N), the site with low groundwater level (S4-D), and site with fluctuating groundwater level (S2-F). Ranges of DBH class are indicated in the Supplementary Material (Table S1)

Tree ID	DBH at installation (cm)	DBH at removal (cm)	DBH class at installation	Change in DBH from installation to removal (cm)	Growth rate throughout study period ( $\text{cm d}^{-1}$ )
S5-T1	10.5	12.7	II	2.2	0.014
S5-T2	10.6	13.1	II	2.5	0.016
S5-T3	11.5	14.8	III	3.3	0.021
S5-T4	9.1	11.2	I	2.1	0.013
S4-T1	6.0	8.0	III	2.0	0.013
S4-T2	6.1	8.6	III	2.5	0.018
S4-T3	7.0	9.9	IV	2.9	0.018
S4-T4	7.5	10.6	IV	3.1	0.018
S2-T1	10.2	13.2	III	3.0	0.020
S2-T2	9.0	11.3	II	2.3	0.015
S2-T3	10.3	12.9	III	2.6	0.016
S2-T4	7.9	10.3	I	2.4	0.015

## Data Analysis and Statistical Tests

### Tree Transpiration

Sap flow raw data were analyzed with the software Sap Flow Tool version 1.5 (ICT International Pty Ltd, Australia). The tree cross-sectional area minus bark depth was assumed as 100% water-conducting. This was assumed after preliminary dye tracer experiments and a regression analysis for determining the water-conducting sapwood depth resulted in negligible differences. Similar assumptions were made in previous studies [15]. Calculated DBH values were inserted manually into the processing software. The results obtained from the software comprised sap velocity, sap flow rate, and daily sap flow.

To derive the tree transpiration ( $T$ , mm) from the sap flow measurements, we used a modification of the approach proposed by Bloemen et al. [13]. Sap flow ( $F_s$ , L) was multiplied by the ratio of the leaf area index of the tree canopy ( $LAI_{canopy}$ ,  $m^2 m^{-2}$ ) to the area of the projected crown ( $A_{crown}$ ,  $m^2$ ):

$$T = F_s * \frac{LAI_{canopy}}{A_{crown}} \quad (1)$$

The crown radius was measured using a measuring tape (1-cm accuracy) both in north–south and east–west directions. The values were then averaged. The area of the projected crown was calculated as a circle with a radius of 2.0 m (for the site with higher groundwater table, S5-N), 1.0 m (for the site with lower groundwater table, S4-D), and 1.8 m (for the site with fluctuating groundwater table, S2-F).

### Statistical Analyses

Differences in the daily mean transpiration among trees and sites were tested with a one-way analysis of variance (ANOVA). Significant differences were analyzed with the Tukey's honestly significant difference (HSD) test using the function "TukeyHSD." A principal component analysis (PCA) with the procedure "prcomp" was performed per site on a matrix that included all measured variables. The matrix consisted of the daily median of all the soil moisture and matric potential sensors, daily mean groundwater level, daily mean air temperature, diurnal cumulative photosynthetic active radiation (PAR), daily mean vapor pressure deficit (VPD), cumulative daily rainfall, and values of mean daily transpiration of the selected trees per site. The aim of a PCA is to reduce the dimensionality of a data set with interrelated variables, with the goal of retaining as much variation of the data set as possible. The resulting set of principal components encompasses most of the variation from the

original variables. The PCA is widely used in meteorology and climatology where large data sets are common [28]. A Pearson's correlation analysis with the function "cor" was used to determine correlations between tree transpiration and meteorological and soil-related variables. All statistical analyses were performed in the statistical software R version 4.0.4 [29] using a level of significance of  $p < 0.05$ .

## Results

### Meteorological Conditions

The weather conditions of the growing season in 2019 were warmer and drier than the long-term averages for the region (Table 1). The total precipitation between the beginning of May and the end of September was 301 mm, with the highest precipitation occurring in May (129 mm). More than 50% of the precipitation recorded for that month occurred during two rainfall events on May 22nd and May 28th. At the same time, PAR exhibited the lowest daily cumulative value on May 22nd ( $117 \text{ mol m}^{-2} \text{ d}^{-1}$ ). In contrast, PAR reached its maximum on June 3rd ( $1514 \text{ mol m}^{-2} \text{ d}^{-1}$ ). Similar values were observed at the beginning of the summer season. Further low PAR values were recorded on September 2nd and 28th ( $165$  and  $176 \text{ mol m}^{-2} \text{ d}^{-1}$ , respectively). These PAR conditions coincided with the lowest values of VPD on May 22nd (0.026 kPa), May 28th (0.0045 kPa), and September 28th (0.045 kPa). Maximum diurnal VPD was reached on July 26th (2.3 kPa). Similar values were also measured on July 6th (2.3 kPa) and July 25th (2.2 kPa). Mean air temperature during the growing season was  $18.2 \text{ }^\circ\text{C}$ ; highest air temperature was  $26.4 \text{ }^\circ\text{C}$  and occurred on June 26th.

### Tree-Based Transpiration

The transpiration results for each monitored tree within the poplar stands in the study area are summarized in Table 4. The results show that on the site with higher groundwater level (S5-N), the tree with the most frequent diameter (S5-T2, DBH class = II) had a daily mean transpiration of  $9.3 \pm 3.7 \text{ mm d}^{-1}$ ; the tree with smaller diameter (S5-T4, DBH class = I) showed a daily mean transpiration of  $5.0 \pm 2.3 \text{ mm d}^{-1}$ , and the tree with the larger diameter (S5-T3, DBH class = III) had a daily mean transpiration of  $11.0 \pm 6.1 \text{ mm d}^{-1}$ . The cumulative growing season transpiration of tree S5-T2 (DBH class = II) was 955 mm, whereas for the tree S5-T4 (DBH class = I), it was 715 mm and for tree S5-T3 (DBH class = III) was 1644 mm. Furthermore, the one-way ANOVA revealed significant differences of the mean daily transpiration rates among the individual trees in this site ( $p < 0.001$ , Table 5). A subsequent Tukey's HSD test indicated a higher mean daily transpiration for

**Table 4** Summary statistics of transpiration values of all monitored trees on the study sites. Site with higher groundwater table (S5-N), site with deeper groundwater table (S4-D), and site with fluctuating groundwater table (S2-F). Monitored trees with a gap in monitoring days larger than 30% of the growing season were excluded from further analysis

Tree ID	Daily transpiration in growing season 2019 (DOY 115–273) (mm)						Data gap (number of days)
	Min	Median	Mean	Max	Standard deviation	Sum total	
S5-T1*	0.002	8.5	7.8	15.2	4.4	717	77
S5-T2*	0.09	10.0	9.3	18.9	3.7	955	39
S5-T3***	−0.07	11.5	10.9	25.6	6.1	1644	18
S5-T4**	−0.19	5.5	5.0	10.3	2.3	715	5
S4-T1*	0.008	3.6	3.0	5.7	1.6	380	41
S4-T2*	0.06	3.4	3.0	5.6	1.5	469	12
S4-T3***	0.056	3.1	2.7	4.9	1.4	330	43
S4-T4***	0.02	10.7	9.3	22.4	5.6	1347	14
S2-T1***	0.12	7.4	7.1	15.8	4.5	810	52
S2-T2*	0.08	6.5	5.9	12.0	3.5	879	16
S2-T3***	0.004	9.1	8.1	14.0	4.0	1012	42
S2-T4**	0.04	5.0	4.5	8.9	2.3	698	5

\*Tree within the most frequent DBH class; \*\*tree within a smaller DBH class; \*\*\*tree within a bigger DBH class

monitored tree S5-T3 (DBH class = III) ( $p=0.01$ , Table 6) than for S5-T2 (DBH class = II) and S5-T4 (DBH class = I) ( $p < 0.001$ , Table 6). However, the tree S5-T2 (DBH class = II) presented a monitoring gap of 39 days; we therefore expect that its transpiration is even higher.

At the site S4-D (low groundwater level), the trees with the most frequent diameter (S4-T1 and S4-T2, DBH class = III) presented a daily transpiration rate of  $3.0 \pm 1.6$  and  $3.0 \pm 1.5$  mm d<sup>−1</sup>. The cumulative transpiration throughout the growing season was 380 mm (S4-T1) and 469 mm (S4-T2). The data gap for tree S4-T1 amounted to 41 days, whereas the gap for the tree S4-T2 (12 days) was the smallest one on the site. The tree within the larger DBH class (S4-T3, DBH class = IV) presented a daily transpiration rate of  $2.7 \pm 1.4$  mm d<sup>−1</sup> and a cumulative transpiration of 330 mm, but with a large data gap of 43 days. The additional monitored tree within the larger DBH class (S4-T4, DBH class = IV) had higher daily transpiration rates ( $9.3 \pm 5.6$  mm d<sup>−1</sup>) and a higher cumulative transpiration for the growing season (1347 mm). The one-way ANOVA revealed significant differences of the mean daily transpiration rates among

the individual trees in this site ( $p < 0.001$ , Table 5). The Tukey's HSD test (Table 6) indicated that the transpiration rate of tree S4-T4 was statistically different from the other three monitored trees on the same site ( $p < 0.001$ ). The analysis did not show any significant differences between trees S4-T1 and S4-T2 ( $p=0.99$ ), S4-T1 and S4-T3 ( $p=0.8$ ), and S4-T2 and S4-T3 ( $p=0.8$ ).

On site S2-F (fluctuating groundwater level), the monitored tree with a diameter within the most frequent DBH class (S2-T2, DBH-class = II) had a daily mean transpiration of  $5.9 \pm 3.5$  mm d<sup>−1</sup> and a cumulative transpiration of 879 mm throughout the growing season (Table 4). The tree with a smaller diameter (S2-T4, DB-class = I) had a lower daily transpiration ( $4.5 \pm 2.3$  mm d<sup>−1</sup>) and a lower cumulative transpiration of 698 mm for the growing season. The tree with a larger diameter (S2-T3, DBH-class = III) had a mean daily transpiration of  $8.1 \pm 4.0$  mm d<sup>−1</sup> and a cumulative transpiration of 1012 mm throughout the growing season. The results of transpiration rates among monitored trees within this site were statistically different ( $p < 0.001$ , Table 5). The Tukey's HSD test revealed significant

**Table 5** Results of the one-way analysis of variance (ANOVA) to test differences in mean daily transpiration rates among the selected trees on site with higher groundwater level (S5-N), site with low groundwater level (S4-D), and site with fluctuating groundwater level (S2-F)

	Degrees of freedom	Sum squares	Mean square	F value	Pr (>F)
Trees in site S5-N	2	3223	1611.4	86.48	<2e-16***
Residuals	1371	25544	18.6		
Trees in site S4-D	3	4334	1444.6	146.5	<2e-16***
Residuals	544	5363	9.9		
Trees in site S2-F	2	882	441.2	40.63	<2e-16***
Residuals	426	4626	10.9		

Significant codes: 0 "\*\*\*\*" 0.001 "\*\*\*\*" 0.01 "\*\*\*\*" 0.05 " ." 0.1 " ." 1

**Table 6** Results of Tukey’s HSD multiple comparison of daily mean transpiration among the selected trees on each of the sites (null hypothesis = means are equal; significance level  $\alpha=0.05$ )

		Mean difference	95% Confidence Interval		Sig	Mean separators
			Lower bound	Upper bound		
Site with higher groundwater level (S5-N)						
Tree T3	Tree T2	1.6	0.3	2.9	0.013	a
Tree T4	Tree T2	-4.3	-5.6	-2.9	0.000	b
Tree T4	Tree T3	-5.9	-7.1	-4.7	0.000	c
Site with low groundwater level (S4-D)						
Tree T2	Tree T1	-0.01	-1.0	1.0	0.99	a
Tree T3	Tree T1	-0.4	-1.9	0.7	0.8	a
Tree T4	Tree T1	6.3	5.3	7.2	0.000	b
Tree T3	Tree T2	-0.35	-1.3	0.6	0.8	a
Tree T4	Tree T2	6.3	5.3	7.2	0.000	b
Tree T4	Tree T3	6.6	5.6	7.6	0.000	b
Site with low groundwater level (S2-F)						
Tree T3	Tree T2	2.2	1.3	3.2	0.000	a
Tree T4	Tree T2	-1.3	-2.2	-0.4	0.001	b
Tree T4	Tree T3	-3.6	-4.4	-2.6	0.000	c

**Table 7** Results of the one-way analysis of variance (ANOVA) to test differences in mean daily transpiration rates among the site with higher groundwater level (S5-N), site with low groundwater level (S4-D), and site with fluctuating groundwater level (S2-F)

	Degrees of freedom	Sum squares	Mean square	F value	Pr (> F)
Site	2	3223	1611.4	86.48	$<2e^{-16}$ ***
Residuals	1371	25544	18.6		

Significant codes: 0 “\*\*\*\*” 0.001 “\*\*\*” 0.01 “\*\*” 0.05 “.” 0.1 “.” 1

differences among the monitored trees ( $p < 0.001$ , Table 6). The transpiration was higher for monitoring tree S2-T3 (DBH-class = III) than S2-T2 (DBH-class = II) and S2-T4 (DBH-class = I).

When comparing among the sites, the ANOVA test indicated statistical differences ( $p < 0.001$ , Table 7). A subsequent Tukey’s HSD test (Table 8) showed larger average transpiration rates for the site with higher groundwater level (S5-N) compared with the other two sites ( $p < 0.001$ ). The site with low groundwater level (S4-D) revealed the lowest

daily transpiration values of all the plots during the growing season ( $p < 0.001$ ).

Transpiration at the site with high groundwater level (S5-N) followed a normal distribution with an observable peak around the mean for all selected trees (Fig. 3). At the site with low groundwater level (S4-D), the distribution was more heterogeneous. Transpiration values were distributed slightly above the mean transpiration rate (3.0 mm d<sup>-1</sup> on average), especially for the trees S4-T1 and S4-T2 (both in DBH class = III). However, an overall a higher occurrence of lower transpiration rates was observed. In contrast to these trees, S4-T4 (DBH class = IV) exhibited very high transpiration values. At the site with fluctuating groundwater level (S2-F), the results were more heterogeneous, indicating a wider distribution of transpiration values. A peak around lower transpiration values was evident on this site. In contrast, negative values were observed at the site with higher groundwater level (S5-N), on the tree with the smallest diameter. This coincides with the recordings of the highest precipitation events at the end of May. Negative values of stem sap flow were observed on the days of other rainfall events on September 7th and 9th. This reverse flow [30] has

**Table 8** Results of Tukey’s HSD multiple comparison of daily mean transpiration among the site with higher groundwater level (S5-N), site with low groundwater level (S4-D), and site with fluctuating groundwater level (S2-F). (Significance level  $\alpha=0.05$ )

		Mean Difference	95% Conf. interval		Sig	Mean separators
			Lower bound	Upper bound		
S5-N	S4-D	3.738	3.070	4.405	0.000	a
S5-N	S2-F	2.312	1.606	3.017	$1e^{-06}$	b
S4-D	S2-F	-1.426	-2.079	-0.774	0.000	c

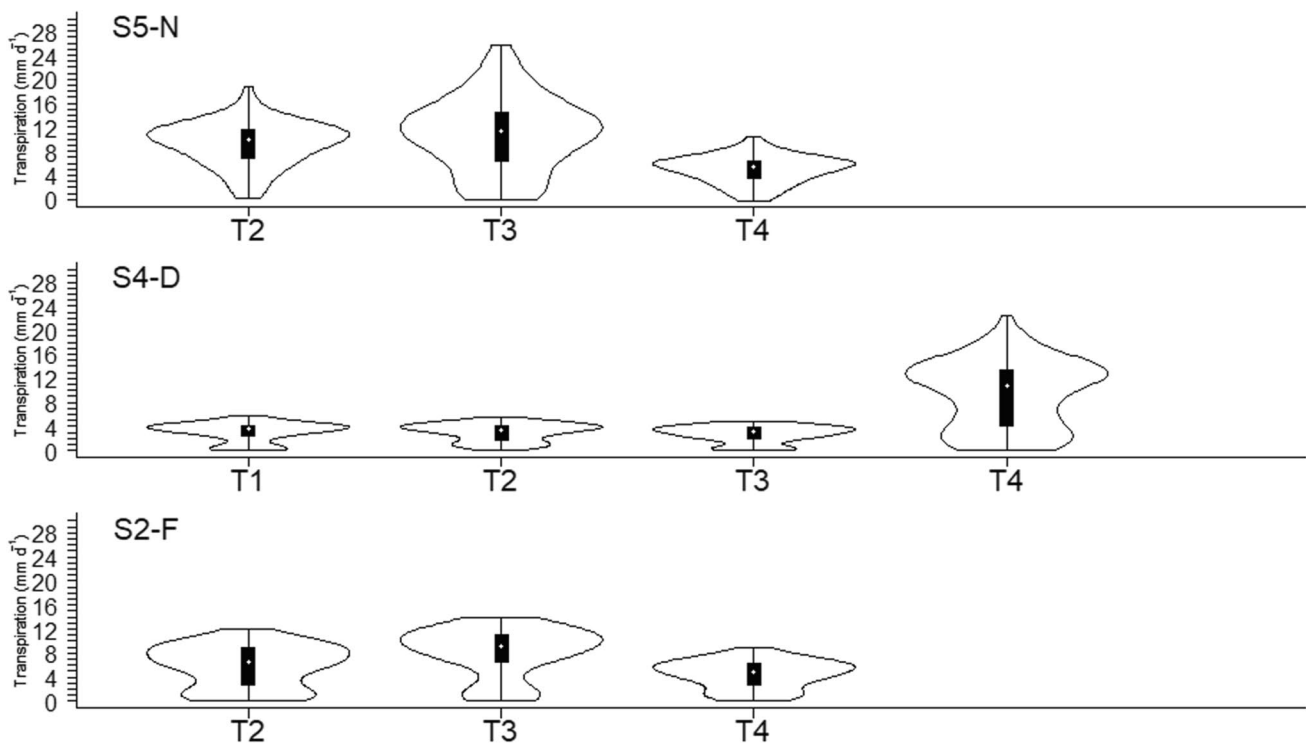


**Fig. 3** Distribution plot of daily mean transpiration (in  $\text{mm d}^{-1}$ ) of monitored trees grouped per site. On the site with higher groundwater level (S5-N), the selected trees were: S5-T2 (DBH class=II), S5-T4, (DBH class=I), and tree S5-T3 (DBH class=III). On the site with low groundwater table (S4-D), the selected trees were S4-T1

(DBH class=III), S4-T2 (DBH class=III), S4-T3 (DBH class=IV), and S4-T4 (DBH class=IV). On the site with fluctuating groundwater level (S2-F), the selected trees were S2-T2 (DBH class=II), S2-T3 (DBH class=III), and S2-T4 (DBH class=I). White dot represents the mean, black bars the standard deviation

been measured with different methods in roots [31, 32] but also in stems. It occurs as result of foliar uptake by frequent dew, fog, or rain events [33]. No other trees, neither in the site with fluctuating groundwater level (S2-F) nor in the site with low groundwater level (S4-D), showed negative transpiration values.

### Transpiration Linked to Meteorological and Soil Conditions

Altogether, transpiration at the site with the higher groundwater level (S5-N) was rather uniform throughout the growing season with values above the mean mainly occurring in July and September, and VPD values exceeding 1.0 kPa. Two large rainfall events on May 22nd and 28th (Fig. 4a) caused an elevated groundwater level. The water table was at its highest on May 30th with 1.60 m below surface, while at the end of the growing season, it was 0.60 m lower. In terms of soil moisture, a rise in the volumetric water content at 30-, 60-, and 90-cm soil depths could be observed. The soil water contents increased to 22.7 vol.-% by the end of May, especially in the deepest layer (Fig. 4d-f). For the following 2 weeks after the precipitation events, the daily mean transpiration of the tree

with the most common diameter (S5-T2, DBH class=II) was  $9.4 \pm 1.0 \text{ mm d}^{-1}$ . The tree with smaller diameter (S5-T4, DBH class=I) showed a daily mean transpiration of  $4.6 \pm 0.7 \text{ mm d}^{-1}$ , and for the tree with the larger diameter (S5-T3, DBH class=III), it was  $10.0 \pm 1.0 \text{ mm d}^{-1}$  within that time period (Fig. 4b). With a relatively dry summer, the values of matric potential started to decrease from the end of June onwards; from July, the curves at 60- and 90-cm soil depth remained relatively constant at a matric potential of pF 3 (Fig. 4e-f). This value is outside the range of plant-available water. Despite this, the daily transpiration rates between July 15th and August 15th were in the order of  $13.5 \pm 2.9 \text{ mm d}^{-1}$  for tree S5-T3 (DBH class=III) and  $6.2 \pm 1.3 \text{ mm d}^{-1}$  for tree S5-T4 (DBH class=I). The daily transpiration rate for tree S5-T2 (DBH class=II) was  $11.3 \pm 3.0 \text{ mm d}^{-1}$  between July 15th and August 5th, when the device failed. Sporadic rainfalls in July and August caused a change from pF 3 to pF 2 in the uppermost 30-cm soil depth; however, they did not cause a noticeable effect on the deeper layers. Two rainfall events on September 7th and 9th increased the water content from 15.2 to 20.3 vol.-% at 30-cm soil depth and from 16.9 to 20.2 vol.-% at 60-cm soil depth (Fig. 4d-e). The highest transpiration rates were observed in September for all

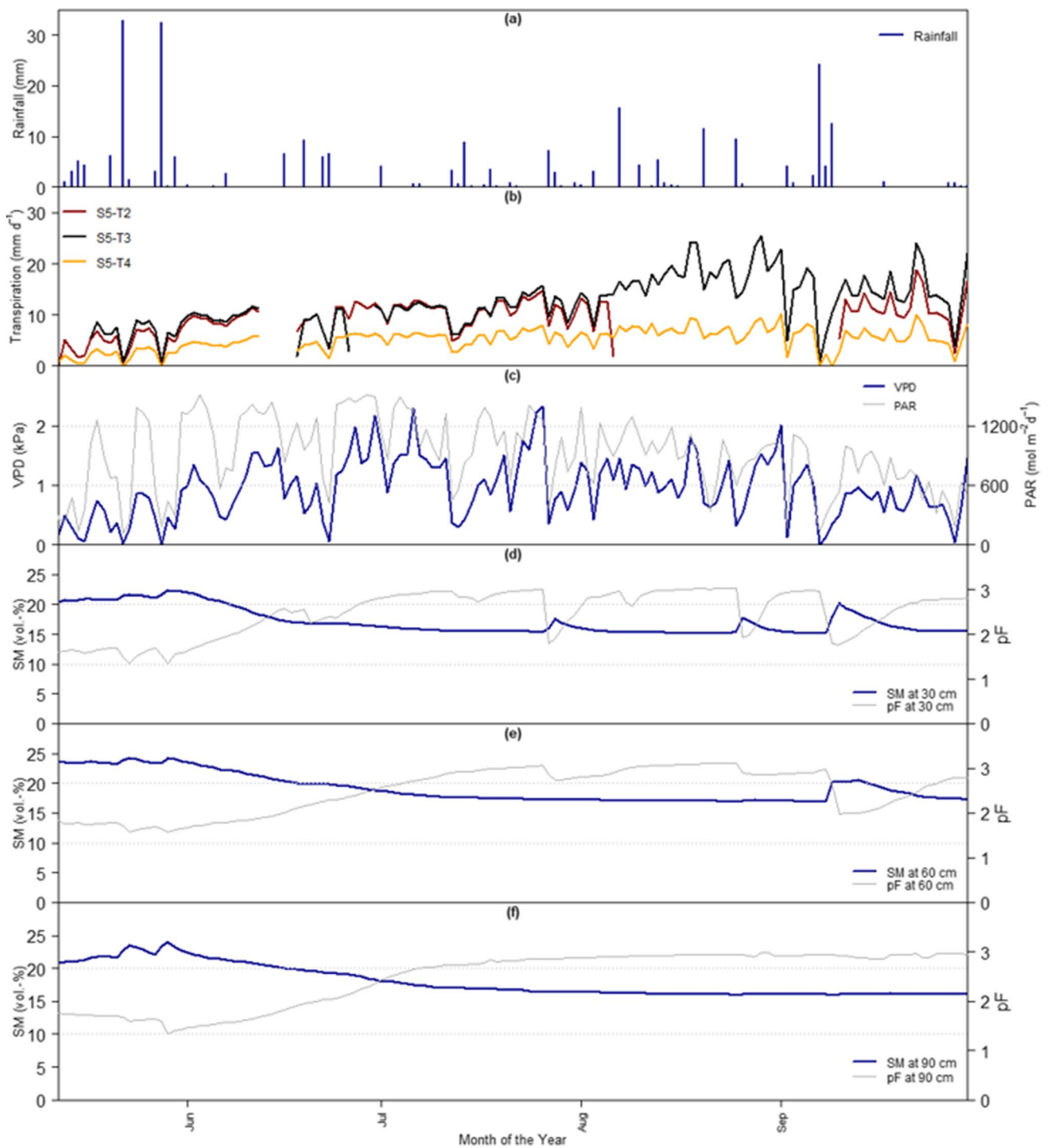


**Fig. 4** Daily mean transpiration in relation to meteorological and soil-related conditions for the site with higher groundwater level (S5-N). **a** Cumulative daily rainfall (mm). **b** Daily course of transpiration ( $\text{mm d}^{-1}$ ) for all the analyzed trees. **c** Daily vapor pressure deficit (VPD, in kPa) and diurnal cumulative photosynthetic active radiation (PAR, in

$\text{mol m}^{-2} \text{d}^{-1}$ ). **d–f** Median daily soil moisture (SM, in vol.-%) (blue line) and median daily matric potential (pF) (gray line) at 30-, 60-, and 90-cm soil depth throughout growing season 2019. Gaps in the daily transpiration curves indicate sensor failure

trees (Fig. 4b, Table 4), except for S5-T3 (DBH class = III) which registered the maximum transpiration on August 29th ( $25.6 \text{ mm d}^{-1}$ ). The lowest values of transpiration

occurred in the beginning of May, both for tree S5-T2 (DBH class = II,  $0.09 \text{ mm d}^{-1}$ ) and the tree S5-T4 (DBH class = I,  $0.27 \text{ mm d}^{-1}$ ). The tree S5-T3 (DBH class = III)

exhibited the lowest transpiration value on September 7th ( $0.66 \text{ mm d}^{-1}$ ). Unfortunately, due to sensor failure, there was a large gap between August 6th and September 9th, which limits our interpretation of water use by clone “AF2” during the growing season on site S5-N (higher groundwater level). The data gap also coincides with the date of maximum LAI ( $6.4 \text{ m}^2 \text{ m}^{-2}$  on August 9th). By September 23rd, LAI was below  $4.0 \text{ m}^2 \text{ m}^{-2}$ .

For the site with low groundwater level (S4-D), soil moisture showed low values ( $8.5 \text{ vol.-%}$ ) at the start of the growing season, especially in the uppermost 30 cm (Fig. 5d). Precipitation events from May (Fig. 5a) replenished this soil layer, registering as an increase in water content to  $19.3 \text{ vol.-%}$  on May 23rd. This condition persisted until a rainfall on May 28th. After this rainfall event the devices malfunctioned, with the exception of S4-T2 (DBH class = III) and S4-T4 (DBH class = IV). During the following days, S4-T2 exhibited a mean daily transpiration of  $2.9 \pm 1.3 \text{ mm d}^{-1}$  until it failed on June 8th. The tree S4-T4 indicated a daily mean transpiration of  $6.4 \pm 1.4 \text{ mm d}^{-1}$  until June 12th when it failed as well (Fig. 5b). By middle of June the soil moisture at 30-cm soil depth exhibited values of  $7.7 \text{ vol.-%}$ , by July 10th, it had reached its minimum at  $5.8 \text{ vol.-%}$  (Fig. 5d). Soil moisture ranged between this value and  $10.6 \text{ vol.-%}$  until the end of the summer. Consequently, soil matric potential exhibited a pF between 2.9 and 3.5 for the same period. In contrast, at 60-cm soil depth, the values ranged between 24.2 and 28.6 vol.-% from bud burst until the middle of June, when a decline was observed until the end of July (Fig. 5e). Volumetric water content stabilized between 15.5 and 16.8 vol.-% until the end of the growing season. Soil water content at 90-cm soil depth exhibited a peak on May 29th ( $18.1 \text{ vol.-%}$ ) and then declined to  $9.1 \text{ vol.-%}$  by the middle of July (Fig. 5f). Between July 15th and August 15th, the trees S4-T1 and S4-T2 (both DBH class = III) exhibited a daily mean transpiration of  $3.9 \pm 0.7 \text{ mm d}^{-1}$  and  $4.1 \pm 0.7 \text{ mm d}^{-1}$ . The tree S4-T3 (DBH class = IV) exhibited a daily mean transpiration of  $3.6 \pm 0.6 \text{ mm d}^{-1}$ . The tree S4-T4 showed a daily mean transpiration of  $13.0 \pm 2.1 \text{ mm d}^{-1}$  during the same period. Maxima were observed on June 26th (S4-T3,  $4.9 \text{ mm d}^{-1}$ ), August 29th (S4-T1,  $5.7 \text{ mm d}^{-1}$ ), September 1st (S4-T4,  $22.0 \text{ mm d}^{-1}$ ), and August 22nd (S4-T2,  $5.6 \text{ mm d}^{-1}$ ) (Fig. 5b, Table 4). Mean groundwater level during the growing season was  $3.3 \pm 0.20 \text{ m}$  below surface. The water table was closest to the surface on June 7th ( $2.8 \text{ m}$  below ground), 1 week after the intense precipitation events in May. By the end of the growing season, groundwater gauges reported a level of  $3.60 \text{ m}$  below ground. In general, LAI values at the site with low groundwater level (S4-D) were lower than at the other two sites. The maximum value of LAI was  $4.8 \text{ m}^2 \text{ m}^{-2}$ , at the beginning of August.

The site with the fluctuating groundwater table (S2-F) exhibited an intermediate behavior between the other two sites. The precipitation events at the end of May (Fig. 6a) caused an increase in soil moisture from  $11.3 \text{ vol.-%}$  at the beginning of the growing season to  $19.7 \text{ vol.-%}$  in the 30 cm layer (Fig. 6d). The increase could be observed in the deeper layers, but to a lower extent at 60-cm soil depth (Fig. 6e) compared to 90 cm, where soil water content reached the highest value ( $27.6 \text{ vol.-%}$ ) on May 31th (Fig. 6f). This was the highest value during the growing season and coincided with a water table located at  $1.20 \text{ m}$  below surface. The daily mean transpiration rates from June 1st until 12th were ranged between  $6.1 \pm 1.2 \text{ mm d}^{-1}$  (S2-T2, DBH-class = II) and  $4.3 \pm 0.6 \text{ mm d}^{-1}$  (S2-T4, DBH-class = I). The sap flow device in S2-T3 (DBH-class = III) did not record any measurements from May 8th to June 18th. From the end of May, there was a sustained decrease in soil moisture during the summer months in the three monitored soil layers. By August 15th, soil moisture had reached  $5.4 \text{ vol.-%}$  at 30-cm soil depth,  $4.2 \text{ vol.-%}$  at 60-cm soil depth, and  $6.4 \text{ vol.-%}$  at 90-cm soil depth (Fig. 6d–f). Despite a drop in soil moisture to  $5.3 \text{ vol.-%}$  on average for all soil depths, and a matric potential between pF 3.4–3.6 (30 cm) and pF 2.6–3.0 (60 cm), the daily mean transpiration from July 15th to August 15th remained high at  $8.8 \pm 1.5 \text{ mm d}^{-1}$  (S2-T2),  $10.0 \pm 1.8 \text{ mm d}^{-1}$  (S2-T3), and  $6.4 \pm 1.2 \text{ mm d}^{-1}$  (S2-T4). Maxima throughout the growing season were observed on July 26th (S2-T3,  $14.0 \text{ mm d}^{-1}$ ), August 18th (S2-T4,  $8.9 \text{ mm d}^{-1}$ ), and September 22nd (S2-T2,  $12.0 \text{ mm d}^{-1}$ ) (Fig. 6b, Table 4).

### Principal Component Analysis

Figure 7 presents the results of the principal component analysis (PCA) for all sites. In the  $x$  and  $y$  axes, the graph shows the variance of the original variables explained by principal components (PC) 1 and 2. In addition, the graph gives an indication of the correlation degree between the variables based on the position of the vector. For instance, volumetric soil water content was very strongly negatively correlated to matric potential (opposite arrows) and negatively correlated to the magnitude of the groundwater level. Soil moisture was larger where the groundwater level was closer to the surface. Jolliffe [28] recommends to select the principal components with an explained variance of the original variables between 70 and 90%. Specifically, on the site with higher groundwater level (S5-N), the cumulative percentage of total variation explained by PC1 and PC2 was 73%. For the site with low groundwater level (S4-D), the cumulative percentage of the total variation explained by PC1 and PC2 was 68%. Therefore, we included a third component (PC3) for further analysis, which explained 11% of the variance. A total variance of 79% was achieved.

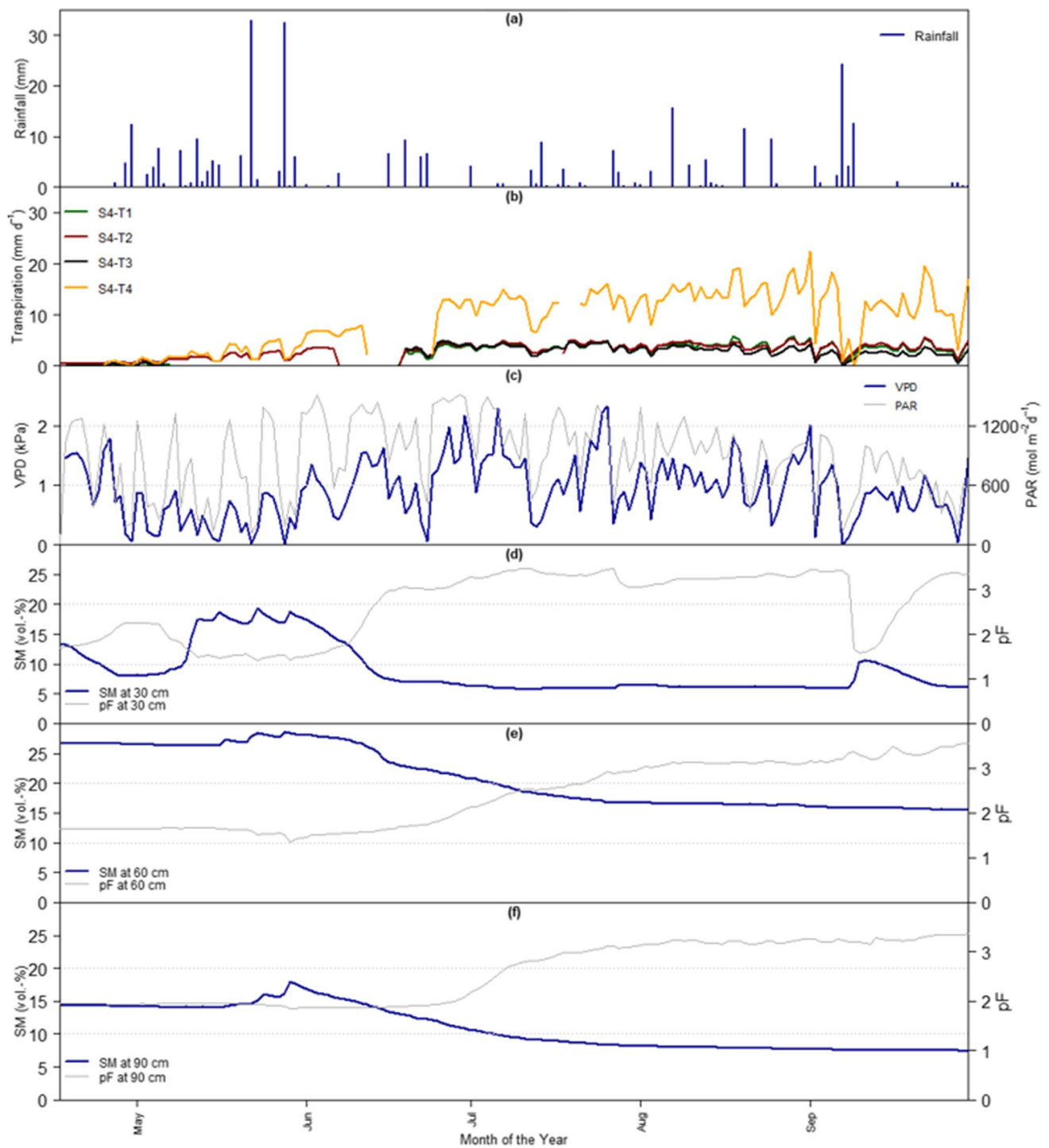


**Fig. 5** Daily mean transpiration in relation to meteorological and soil-related conditions for the site with low groundwater level (S4-D). **a** Cumulative daily rainfall (mm). **b** Daily course of transpiration (mm d<sup>-1</sup>) for all the analyzed trees within the site. **c** Daily vapor pressure deficit (VPD, in kPa) and diurnal cumulative photosynthetic active

radiation (PAR, in mol m<sup>-2</sup> d<sup>-1</sup>). **d-f** Median daily soil moisture (SM, in vol.-%) (blue line) and median daily matric potential (pF) (gray line) at 30-, 60-, and 90-cm soil depth throughout growing season 2019. Gaps in the daily transpiration curves indicate sensor failure

For the site with fluctuating groundwater level (S2-F), the cumulative percentage of total variation explained by PC1 and PC2 was 75%. Table 9 indicates the loadings for each

variable per selected component and site. The loadings with a higher magnitude show the weight of the original variable in determining the PC. For site S5-N (with higher

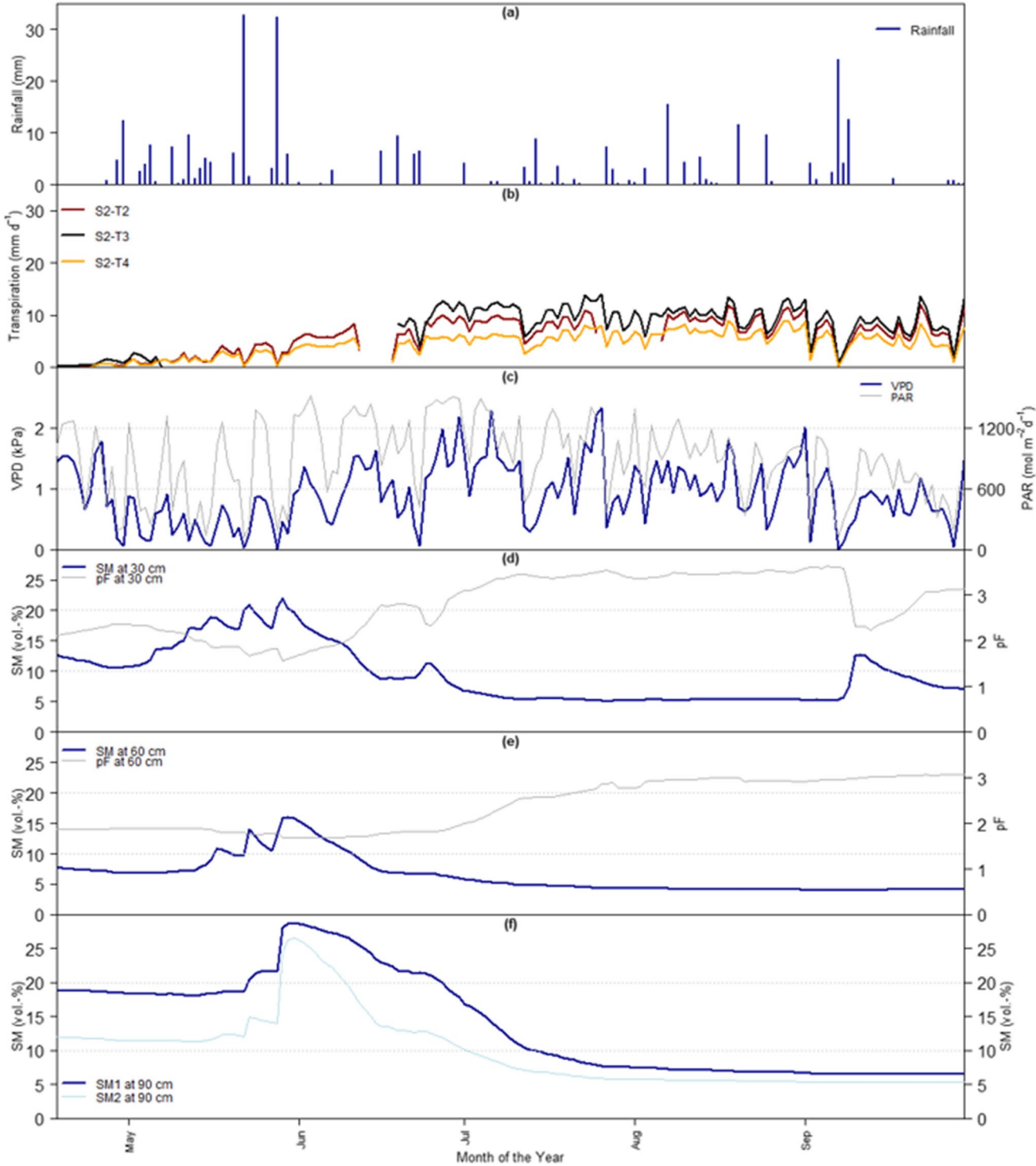


**Fig. 6** Daily mean transpiration in relation to meteorological and soil-related conditions for the site with fluctuating groundwater level (S2-F). **a** Cumulative daily rainfall (mm). **b** Daily mean transpiration ( $\text{mm d}^{-1}$ ) for all the analyzed trees within the site. **c** Vapor pressure deficit (VPD, in kPa) and diurnal cumulative photosynthetic active radia-

tion (PAR, in  $\text{mol m}^{-2} \text{d}^{-1}$ ). **d-f** Median daily soil moisture (SM, in vol.-%) (blue line) and median daily matric potential (pF) (gray line) at 30-, 60-, and 90-cm soil depth throughout growing season 2019. Gaps in the daily transpiration curves indicate sensor failure

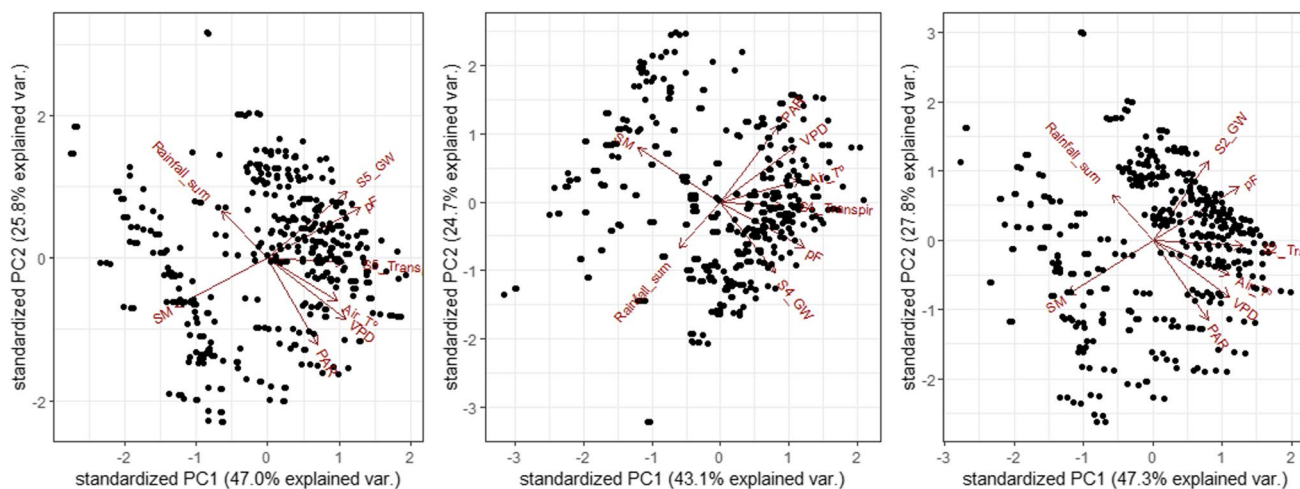


**Fig. 7** Results of principal component analysis (PCA) for the site with higher groundwater level (S5-N, left), for the site with low groundwater level (S4-D, center), and for the site with fluctuating groundwater level (S2-F, right) including variance per principal components (PC) 1 and 2. Analyzed variables included daily mean groundwater level (GW), daily median of all the sensors of soil mois-

ture at 30-, 60-, and 90-cm soil depths (SM), daily median of all the sensors of matric potential at 30-, 60-, and 90-cm soil depths (pF), daily mean transpiration of all selected trees (Transpir.), daily mean air temperature (Air T°), daily mean vapor pressure deficit (VPD), diurnal cumulative photosynthetic active radiation (PAR), and cumulative rainfall (Rainfall\_sum)

**Table 9** Loadings for each meteorological and soil-related variables per principal component (PC) for the site with higher groundwater level (S5-N), site with low groundwater level (S4-D), and site with fluctuating groundwater level (S2-F). Analyzed variables included daily mean transpiration of all selected trees (transpiration), cumulative rainfall (rainfall), daily mean groundwater level (GW), daily

mean air temperature (air temperature), daily mean vapor pressure deficit (VPD), diurnal cumulative photosynthetic active radiation (PAR), daily median of all the sensors of soil moisture at 30-, 60-, and 90-cm soil depths (SM), daily median of all the sensors of matric potential at 30-, 60-, and 90-cm soil depths (pF)

Variable	Loadings per component per site							
	S5-N		S4-D			S2-F		
	PC1	PC2	PC1	PC2	PC3	PC1	PC2	
Transpiration	0.36	-0.03	0.31	-0.02	0.05	0.44	-0.04	
Rainfall	-0.22	0.30	-0.21	-0.31	-0.81	-0.20	0.29	
GW	0.38	0.43	0.28	-0.48	0.30	0.27	0.50	
Air temperature	0.33	-0.27	0.41	0.14	-0.48	0.37	-0.22	
VPD	0.37	-0.39	0.39	0.38	-0.05	0.37	-0.36	
PAR	0.24	-0.55	0.30	0.52	-0.08	0.27	-0.51	
SM	-0.44	-0.31	-0.43	0.37	-0.04	-0.42	-0.35	
pF	0.44	0.32	0.43	-0.31	-0.11	0.42	0.34	

groundwater level), the variables with high loadings in PC1 were soil moisture, matric potential, groundwater, and VPD. In contrast, for PC2, the variables with a higher contribution were PAR, groundwater, and VPD. For the site with low groundwater level (S4-D), the variables contributing to PC1 were soil moisture, matric potential, and the meteorological variables air temperature and VPD. In PC2, we observed a high contribution of PAR, VPD, and groundwater. PC3 had high loadings for the variables rainfall and groundwater. For the site with fluctuating groundwater level (S2-F), high loadings were observed in soil moisture, matric

potential, air temperature, and VPD in PC1. For PC2, the variables with high loadings were PAR, groundwater, air temperature, and soil moisture. The comparison among the sites revealed soil moisture, matric potential, and VPD to be common variables, appearing in PC1 for all sites. The variable groundwater, however, showed a higher loading only for the site with high groundwater level (S5-N) and not for the other two sites. For PC2, the meteorological variables, namely PAR and VPD, indicated high loadings for all three sites, followed by the groundwater variable for all three sites.

## Pearson's Correlation Analysis

The results of Pearson's correlation analysis between daily mean transpiration and the meteorological (air temperature, rainfall, VPD, PAR) and soil-related site variables (groundwater, soil moisture, and matric potential) were statistically significant ( $p < 0.001$ , Table 10). Specifically at the site with higher groundwater level (site S5-N), transpiration was negatively correlated to soil moisture ( $r = -0.45$ ) and positively correlated with the numerical value of pF ( $r = 0.46$ ). In addition, groundwater level (in meters below surface) and daily transpiration showed a positive correlation ( $r = 0.48$ ). The correlation coefficients for the meteorological variables, namely VPD and air temperature, were strong ( $r = 0.46$ ) to moderate ( $r = 0.38$ ). For the site with low groundwater level (S4-D), the correlation coefficients were weak for all analyzed variables. The highest correlation coefficient was found between transpiration and air temperature ( $r = 0.37$ ), followed by matric potential ( $r = 0.34$ ) and VPD ( $r = 0.33$ ). Pearson's correlation test for the site with fluctuating groundwater (S2-F) revealed moderate correlations for air temperature ( $r = 0.62$ ) and matric potential ( $r = 0.62$ ). A moderate correlation was also found for VPD ( $r = 0.57$ ) and soil moisture ( $r = -0.59$ ).

**Table 10** Pearson's correlation test among daily mean transpiration values and meteorological and soil-related variables for the site with higher groundwater level (S5-N), the site with low groundwater level (S4-D), and the site with fluctuating groundwater level (S2-F). Meteorological variables included cumulative rainfall, daily mean groundwater level, daily mean air temperature, daily mean vapor pressure deficit (VPD), and diurnal cumulative photosynthetic active radiation (PAR). Site variables included daily median of all the sensors of soil moisture at 30-, 60-, and 90-cm soil depths (SM), and daily median of all the sensors of matric potential at 30-, 60-, and 90-cm soil depths (pF)

Variable	Daily mean transpiration per site		
	S5-N	S4-D	S2-F
Daily transpiration	1	1	1
Rainfall	-0.30 ****	-0.17 ****	-0.29 ****
Groundwater	0.48 ****	0.32 ****	0.37 ****
Air Temperature	0.38 ****	0.37 ****	0.62 ****
VPD	0.46 ****	0.33 ****	0.57 ****
PAR	0.27 ****	0.24 ****	0.44 ****
SM	-0.45 ****	-0.31 ****	-0.59 ****
pF	0.46 ****	0.34 ****	0.62 ****

$p < .0001$  "\*\*\*\*";  $p < .001$  "\*\*\*\*";  $p < .01$  "\*\*\*";  $p < .05$  "\*\*"

## Discussion

### Water Use by Hybrid Poplar "AF2" in Sites with Contrasting Groundwater Accessibility

The transpiration rates of the monitored trees at the three study sites with contrasting groundwater availability showed significant differences, confirming our research hypotheses. The results from the sites with fluctuating groundwater level (S2-F) and with low groundwater level (S4-D) compare well with the studies listed by Fischer et al. [10] and studies with other poplar clones [8, 12, 17], conducted in soils with similar texture and groundwater levels as our study sites. The mean and maximum daily rates at the site with higher groundwater level (S5-N) were moderately larger. The soil texture in all three experimental plots was comparable. All plots were categorized as loamy sand, with a sand-fraction  $> 70$  mass-% at the site with higher groundwater level (S5-N), 87 mass-% at the site with low groundwater level (S4-D), and 83 mass-% at the site with fluctuating groundwater level (S2-F) (Table 2). The silt proportion was higher at the three evaluated depths at the site S5-N (higher groundwater level), possibly causing an improved water retention capacity. The clay content at site S4-D (low groundwater level), at 60-cm soil depth, was 8.2 mass-%, higher than at 30 cm (4.2 mass-%) and at 90 cm (5.3 mass-%) (Table 2). Such clay bands are frequently found in sandy fluvial deposits and result in an increased water-holding capacity or accumulation of water infiltrating from the upper soil layers.

The average cumulative transpiration of the monitored trees at the site with a higher groundwater level (S5-N, 1105 mm) was larger than at the site with a lower groundwater level (S4-D, 632 mm) and the site with fluctuating groundwater (S2-F, 863 mm) as indicated in Table 4. In general, there are still constraints for scaling from tree to stand transpiration by means of sap flow techniques [34]. The calculations can vary greatly depending on the chosen method [35], but also due to different tree size (Table 5, Table 6). Our results provide a basis for future studies on scaling water use by hybrid poplars to stand level. As tree grow in diameter, their water use may increase [18]. Therefore, the consideration of diameter size classes used in this research and in previous studies [8, 17] yields more reliable results about water fluxes and water budget calculations.

Some trees had larger gaps in the sap flow measurements; therefore, it seems plausible that transpiration in the study area could be even higher. Besides soil moisture, transpiration can also be sustained by tree roots with access to groundwater during dry periods. Previous research with hybrid poplars have demonstrated that water use may

increase with greater water availability and greater above- and belowground biomass [15]. Another study reported rooting depths of up to 2.5 m (below surface) for 5-year-old poplars [12]. Other authors have found access of poplar roots to shallow groundwater reservoirs (1.3 to 2.0 m depth) [16, 36]. It is conceivable that at our study sites, the planted clone “AF2” has reached the groundwater table and is using groundwater as additional water supply. At the site with low groundwater table (S4-D), trees may have found favorable conditions with regard to plant-available water supply in deeper soil depths (60 cm).

### Transpiration Linked to Meteorological and Other Site Conditions

The results of the PCA and the correlation analysis indicate a relation between transpiration and meteorological (especially VPD and PAR) and soil-related variables (soil moisture, matric potential, and groundwater). These results support our hypotheses and agree with studies in which meteorological and soil-related conditions were monitored. Other studies mainly reported positive correlations between transpiration dynamics, VPD and PAR [17], in areas with high groundwater level [16]. Petzold et al. [8] deemed site conditions, especially soil water availability and soil temperature, to be controlling variables for transpiration. Our results demonstrate that the contribution of meteorological and soil-related variables to transpiration differed among sites. We initially hypothesized that the influence of meteorological conditions would be limited by the different soil-related site characteristics. That assumption was based on the presence of more favorable soil moisture conditions and better groundwater accessibility at the site with higher groundwater level (S5-N). Consequently, soil water would not be a limiting factor, and transpiration would only be determined by the evaporative demand of the atmosphere. Therefore, the higher groundwater level explains the transpiration rates. Meanwhile, soil water was the limiting factor for transpiration for the site with low groundwater level (S4-D). We found that mainly soil moisture and matric potential explained the variance in transpiration. In the Pearson’s correlation analysis, VPD was more closely related to transpiration rates only for the sites with higher (S5-N) and with fluctuating groundwater (S2-F). Thus, we can conclude that for environments with optimal water conditions, soil-related site and meteorological conditions determine the transpiration rate to a similar degree. For drier areas, soil water availability controls the transpiration rates. More experimental studies considering the entire soil–plant–atmosphere continuum would help to gain a better understanding of the transpiration process, helped further by the use of stable isotopes to determine sources for tree water uptake [37] and genotype-specific water use efficiency [6].

The increase in diameter for the monitored genotype was similar for all study sites at the end of the growing season (Table 3), suggesting that the clone “AF2” found optimal conditions in terms of water supply, from either soil water, groundwater, or both. The growth of the planted trees was not affected by the rainless summer. This indicates the generalist behavior of the studied hybrid [38]. Regardless of the low observed values of soil matric potential, soil water was available for the trees to maintain their physiological activity. Di Matteo et al. [39] found higher values of stomatal conductance for the clone “AF2” during summer drought, indicating that it would be a suitable hybrid for cultivation in drier conditions where water is limited. Furthermore, the authors found high intrinsic water use efficiency and high yields by the same clone. Heilig et al. [40] also concluded that *Populus deltoides* × *P. nigra* are less susceptible to water stress and tend to develop well when water conditions are optimal. The genotype “AF2” seems to have met its water requirements at the study sites with sand-dominated soil and with low water-holding capacity in the Moravian floodplains. Our research has shown that soil water availability and groundwater accessibility are critical for biomass production at our study sites. In scenarios of a changing climate, where summer droughts like in 2019 might occur more frequently, both site and plant material selection are crucial (cf. [12, 38]) and have implications for growth. Adapting the rotation duration or plantation density [18] may have desirable effects when seeking high productive potential [41] or dealing with site-specific changes in water fluxes [19]. On sites where trees may reach the groundwater, potential impacts on local water balance should be closely monitored.

### Conclusions

The present study determined transpiration rates in the clone “AF2” in SRC stands on sand-dominated soils with contrasting groundwater accessibility in western Slovakia for the growing season 2019. Transpiration rates were statistically different among the sites and relatively constant throughout the growing season. On the site with a higher groundwater level, tree water use was higher and sustained by the shallow groundwater reservoir. Meanwhile, at the site with low groundwater level, transpiration was limited by soil water availability. Regardless of the location, the clone “AF2” exhibited same diameter increases during the growing season. The SRC plantations with the genotype *Populus deltoides* Bart. ex Marsh × *P. nigra* L. “AF2” in Moravian floodplains with predominantly sandy soils and a low amount of plant-available water have fulfilled their water requirements. In general, our results indicate that degraded or abandoned land with an optimal water supply could potentially be cultivated with hybrid poplars as short rotation coppices. As our study demonstrates, water use can

vary within a small area due to factors like texture-related soil moisture dynamics or groundwater accessibility. Considering combined site conditions is therefore crucial for the implementation of sustainable SRC systems.

**Supplementary Information** The online version contains supplementary material available at <https://doi.org/10.1007/s12155-022-10445-x>.

**Acknowledgements** The authors gratefully acknowledge the support of Hanna Teuchert, Ann Kamamia, Robert Rasch, Tobias Stefan, and Matthias Hacker during field work.

**Funding** Open Access funding enabled and organized by Projekt DEAL. This study has been supported by the Bio Based Industries Joint Undertaking under the European Union's Horizon 2020 research and innovation program under grant agreement No 745874 "Dendromass for Europe" (D4EU).

**Data availability** The raw data is proprietary but can be disclosed by sending a motivated request to the corresponding author.

## Declarations

**Ethics Approval** This study did not include human or animal testing.

**Consent to Participate** All individuals involved with the experiment were informed about the study purpose and methods and agreed to participate.

**Consent for Publication** All partners agreed with publication in the present form.

**Conflict of Interest** The authors declare no competing interests.

**Open Access** This article is licensed under a Creative Commons Attribution 4.0 International License, which permits use, sharing, adaptation, distribution and reproduction in any medium or format, as long as you give appropriate credit to the original author(s) and the source, provide a link to the Creative Commons licence, and indicate if changes were made. The images or other third party material in this article are included in the article's Creative Commons licence, unless indicated otherwise in a credit line to the material. If material is not included in the article's Creative Commons licence and your intended use is not permitted by statutory regulation or exceeds the permitted use, you will need to obtain permission directly from the copyright holder. To view a copy of this licence, visit <http://creativecommons.org/licenses/by/4.0/>.

## References

- European Commission A European Green Deal | European Commission. [https://ec.europa.eu/info/strategy/priorities-2019-2024/european-green-deal\\_en#documents](https://ec.europa.eu/info/strategy/priorities-2019-2024/european-green-deal_en#documents). Accessed 31 May 2021
- Sikkema R, Proskurina S, Banja M, Vakkilainen E (2021) How can solid biomass contribute to the EU's renewable energy targets in 2020, 2030 and what are the GHG drivers and safeguards in energy- and forestry sectors? *Renew Energy* 165:758–772. <https://doi.org/10.1016/j.renene.2020.11.047>
- Meyer M, Tavares Wahren F, Weber N, Zalesny RS, Weih M (2021) Sustainable biomass value chains based on poplar plantations in European rural areas. *Bioenergy Res*. <https://doi.org/10.1007/s12155-021-10275-3>
- Bioenergy Europe (2019) Biomass for energy: agricultural residue and energy crops. *Bioenergy Explain*. <https://bioenergyeurope.org/article/204-bioenergy-explained-biomass-for-energy-agricultural-residues-energy-crops.html>. Accessed 20 June 2021
- Štochlová P, Novotná K, Costa M, Rodrigues A (2019) Biomass production of poplar short rotation coppice over five and six rotations and its aptitude as a fuel. *Biomass Bioenergy* 122:183–192. <https://doi.org/10.1016/j.biombioe.2019.01.011>
- Zalesny RS, Stanturf JA, Gardiner ES, Perdue JH, Young TM, Coyle DR, Headlee WL, Bañuelos GS, Hass A (2016) Ecosystem services of woody crop production systems. *Bioenergy Res* 9:465–491
- Dimitriou L, Busch G, Jacobs S, Schmidt-Walter P, Lamersdorf N (2009) A review of the impacts of short rotation coppice cultivation on water issues. *Landbauforsch Volkenrode* 59:197–206
- Petzold R, Schwärzel K, Feger K-H (2011) Transpiration of a hybrid poplar plantation in Saxony (Germany) in response to climate and soil conditions. *Eur J For Res* 130:695–706. <https://doi.org/10.1007/s10342-010-0459-z>
- King JS, Ceulemans R, Dillen SY, Domec JC, Fichot R, Fischer M, Leggett Z, Sucre E, Trnka M, Zenone T (2013) The challenge of lignocellulosic bioenergy in a water-limited world. *Bioscience* 63:102–117. <https://doi.org/10.1525/bio.2013.63.2.6>
- Fischer M, Trnka M, Kučera J, Deckmyn G, Orság M, Sedlák P, Žalud Z, Ceulemans R (2013) Evapotranspiration of a high-density poplar stand in comparison with a reference grass cover in the Czech-Moravian Highlands. *Agric For Meteorol* 181:43–60. <https://doi.org/10.1016/j.agrformet.2013.07.004>
- Frédette C, Labrecque M, Comeau Y, Brisson J (2019) Willows for environmental projects: a literature review of results on evapotranspiration rate and its driving factors across the genus *Salix*. *J Environ Manage* 246:526–537. <https://doi.org/10.1016/j.jenvman.2019.06.010>
- Schmidt-Walter P, Richter F, Herbst M, Schuldt B, Lamersdorf NP (2014) Transpiration and water use strategies of a young and a full-grown short rotation coppice differing in canopy cover and leaf area. *Agric For Meteorol* 195–196:165–178. <https://doi.org/10.1016/j.agrformet.2014.05.006>
- Bloemen J, Fichot R, Horemans JA, Broeckx LS, Verlinden MS, Zenone T, Ceulemans R (2017) Water use of a multigenotype poplar short-rotation coppice from tree to stand scale. *GCB Bioenergy* 9:370–384. <https://doi.org/10.1111/gcbb.12345>
- Meiresonne L, Nadezhdin N, Cermak J, Van Slycken J, Ceulemans R (1999) Measured sap flow and simulated transpiration from a poplar stand in Flanders (Belgium). *Agric For Meteorol* 96:165–179. [https://doi.org/10.1016/S0168-1923\(99\)00066-0](https://doi.org/10.1016/S0168-1923(99)00066-0)
- Zalesny RS, Wiese AH, Bauer EO, Riemenschneider DE (2006) Sapflow of hybrid poplar (*Populus nigra* L. × *P. maximowiczii* A. Henry 'NM6') during phytoremediation of landfill leachate. *Biomass Bioenergy* 30:784–793. <https://doi.org/10.1016/j.biombioe.2005.08.006>
- Zhang H, Morison JIL, Simmonds LP (1999) Transpiration and water relations of poplar trees growing close to the water table. *Tree Physiol* 19:563–573. <https://doi.org/10.1093/treephys/19.9.563>
- Navarro A, Portillo-Estrada M, Arriga N, Vanbeveren SPP, Ceulemans R (2018) Genotypic variation in transpiration of coppiced poplar during the third rotation of a short-rotation bio-energy culture. *GCB Bioenergy* 10:592–607. <https://doi.org/10.1111/gcbb.12526>
- Renninger HJ, Stewart LF, Rousseau RJ (2021) Water use, efficiency, and stomatal sensitivity in eastern cottonwood and hybrid poplar varieties on contrasting sites in the Southeastern United States. *Front For Glob Chang* 4:1–16. <https://doi.org/10.3389/ffgc.2021.704799>

19. Wahren A, Richter F, Julich S, Jansen M, Feger K-H (2015) The influence of more widespread cultivation of short rotation coppice on the water balance: from the site to the regional scale. In: Butler-Manning D, Bemmman A, Bredemeier M, Lamersdorf NP, Ammer C (eds) *Bioenergy from dendromass for the sustainable development of rural areas*, First edn. Wiley-VCH Verlag GmbH & Co. KGaA, Weinheim, pp 45–61
20. Richter F, Döring C, Jansen M, Panferov O, Spank U, Bernhofer C (2015) How to predict hydrological effects of local land use change: how the vegetation parameterisation for short rotation coppices influences model results. *Hydrol Earth Syst Sci* 19:3457–3474. <https://doi.org/10.5194/hess-19-3457-2015>
21. Climate-Data.org. <https://de.climate-data.org/europa/slowakei/tyrnauer-landschaftsverband/holitsch-7263/>. Accessed 5 May 2020
22. Hartmann K (2010) *Entwicklung eines Ertragsschätzers für Kurzumtriebsbestände aus Pappel*. Dissertation. Technische Universität Dresden. <https://nbn-resolving.org/urn:nbn:de:bsz:14-qucosa-62853>
23. Burgess SSO, Adams MA, Turner NC, Beverly CR, Ong CK, Khan AAH, Bleby TM (2001) An improved heat pulse method to measure low and revers rates of sap flow in woody plants. *Tree Physiol* 21:589–598
24. Burgess S, Downey A, International ICT (2014) *SFM1 Sap Flow Meter Manual*. <https://ictinternational.com/content/uploads/2014/03/SFM1-Manual-v5-1.pdf>
25. Martínez-Vilalta J, Mangirón M, Ogaya R, Sauret M, Serrano L, Peñuelas J, Piñol J (2003) Sap flow of three co-occurring Mediterranean woody species under varying atmospheric and soil water conditions. *Tree Physiol* 23:747–758. <https://doi.org/10.1093/treephys/23.11.747>
26. Gascon F, Bouzinac C, Thépaut O, Jung M, Francesconi B, Louis J, Lonjou V, Lafrance B, Massera S, Gaudel-Vacaresse A, Languille F, Alhammoud B, Viallefont F, Pflug B, Bieniarz J, Clerc S, Pessiot L, Trémas T, Cadau E, De Bonis R, Isola C, Martimort P, Fernandez V (2017) Copernicus sentinel-2A calibration and products validation status. *Remote Sens* 9. <https://doi.org/10.3390/rs9060584>
27. Agency ES Sentinel-2 SNAP toolbox. <http://step.esa.int/main/toolboxes/sentinel-2-toolbox>. Accessed 15 Mar 2021
28. Jolliffe IT (2002) *Principal component analysis*, 2nd edn. Springer
29. R Core Development Team (2018) *R: A language and environment for statistical computing*. R Foundation for Statistical Computing, Vienna, Austria. URL <https://www.R-project.org/>
30. Burgess SSO, Adams MA, Turner NC, Ong CK (1998) The redistribution of soil water by tree root systems. *Oecologia* 115:306–311. <https://doi.org/10.1007/s004420050521>
31. David TS, Pinto CA, Nadezhkina N, Kurz-Besson C, Henriques MO, Quilhó T, Cermak J, Chaves MM, Pereira JS, David JS (2013) Root functioning, tree water use and hydraulic redistribution in *Quercus suber* trees: a modeling approach based on root sap flow. *For Ecol Manage* 307:136–146. <https://doi.org/10.1016/j.foreco.2013.07.012>
32. Prieto I, Armas C, Pugnaire FI (2012) Water release through plant roots: New insights into its consequences at the plant and ecosystem level. *New Phytol* 193:830–841. <https://doi.org/10.1111/j.1469-8137.2011.04039.x>
33. Limm EB, Simonin KA, Bothman AG, Dawson TE (2009) Foliar water uptake: a common water acquisition strategy for plants of the redwood forest. *Oecologia* 161:449–459. <https://doi.org/10.1007/s00442-009-1400-3>
34. Lundblad M, Lindroth A (2002) Stand transpiration and sapflow density in relation to weather, soil moisture and stand characteristics. *Basic Appl Ecol* 3:229–243. <https://doi.org/10.1078/1439-1791-00099>
35. Wang D, Gao G, An J, Shao Y, Lü Y, Fu B (2022) Comparisons of three scaling up methods to estimate stand transpiration of a xerophytic shrub (*Salix psammophila*) in northern China. *J Hydrol* 608:127593. <https://doi.org/10.1016/J.JHYDROL.2022.127593>
36. Migliavacca M, Meroni M, Manca G, Matteucci G, Montagnani L, Grassi G, Zenone T, Teobaldelli M, Godeo I, Colombo R, Seufert G (2009) Seasonal and interannual patterns of carbon and water fluxes of a poplar plantation under peculiar eco-climatic conditions. *Agric For Meteorol* 149:1460–1476. <https://doi.org/10.1016/j.agrformet.2009.04.003>
37. Jackisch C, Knoblauch S, Blume T, Zehe E, Hassler SK (2020) Estimates of tree root water uptake from soil moisture profile dynamics. *Biogeosciences* 17:5787–5808. <https://doi.org/10.5194/bg-17-5787-2020>
38. Truax B, Gagnon D, Fortier J, Lambert F (2014) Biomass and volume yield in mature hybrid poplar plantations on temperate abandoned farmland. *Forests* 5:3107–3130. <https://doi.org/10.3390/f5123107>
39. Di Matteo G, Nardi P, Verani S, Sperandio G (2015) Physiological adaptability of Poplar clones selected for bioenergy purposes under non-irrigated and suboptimal site conditions: a case study in Central Italy. *Biomass Bioenergy* 81:183–189. <https://doi.org/10.1016/j.biombioe.2015.06.023>
40. Heilig D, Heil B, Leibing C, Röhle H, Kovács G (2021) Comparison of the Initial Growth of different poplar clones on four sites in western Slovakia—preliminary results. *Bioenergy Res* 14:374–384. <https://doi.org/10.1007/s12155-020-10227-3>
41. Di Matteo G, Sperandio G, Verani S (2012) Field performance of poplar for bioenergy in southern Europe after two coppicing rotations: effects of clone and planting density. *IForest* 5:224–229. <https://doi.org/10.3832/ifor0628-005>

**Publisher's Note** Springer Nature remains neutral with regard to jurisdictional claims in published maps and institutional affiliations.